Original Article

Effects of collimated and focused low-intensity pulsed ultrasound stimulation on the mandible repair in rabbits

Xiaohan Liu[1], Ying Hu[2], Lin Wu[1], Shujun Li[3]

[1]Department of Prosthodontics, School and Hospital of Stomatology, China Medical University, Liaoning Provincial Key Laboratory of Oral Diseases, Shenyang 110002, China; [2]Department of Pediatric Dentistry, Dalian Stomatological Hospital, Dalian 116021, China; [3]Shenyang National Laboratory for Materials Science, Institute of Metal Research, Chinese Academy of Sciences, Shenyang 110016, China

Contributions: (I) Conception and design: L Wu; (II) Administrative support: X Liu, L Wu; (III) Provision of study materials or patients: S Li; (IV) Collection and assembly of data: Y Hu; (V) Data analysis and interpretation: X Liu; (VI) Manuscript writing: All authors; (VII) Final approval of manuscript: All authors.

Correspondence to: Lin Wu. Department of Prosthodontics, China Medical University School of Stomatology, Shenyang 110002, China. Email: wulin13@163.com.

Background: This study was to evaluate the effects of low-intensity collimated pulse ultrasound (LICU) and low-intensity focused-pulse ultrasound (LIFU) stimulation on the osteogenesis in the porous silicon carbide (SiC) scaffold implanted in the rabbit mandible.

Methods: Rabbits were randomly divided into LIFU group, LICU group and control group (without ultrasound treatment). The intensities of LICU and LIFU were 30 and 300 mW/cm^2, respectively. The subcutaneous and subperiosteal temperatures were measured continuously during the 20-min ultrasound treatment. Then, the porous SiC scaffolds were implanted into the mandible, followed by LICU or LIFU once daily, and the quantity and structure of bone were assessed by methylene blue-acid fuchsin staining and micro-CT at 3, 6 and 9 weeks after implantation.

Results: The changes in the subcutaneous and subperiosteal temperatures during LICU and LIFU were less than 1 ℃. The bone mass increased and the structure of bone tissues became more mature over time. The bone mass and mean pore occupancy fraction (POF) in the LIFU group were significantly greater than in the LICU group at three time points ($P<0.05$). Bone ingrowth in different directions was observed, and the new bone formation in the mesial, distal, top, and lingual sides of the implants in the LIFU group was greater than in the LICU group and control group ($P<0.05$).

Conclusions: LIFU and LICU may effectively promote bone formation in the mandible scaffold, and LIFU significantly accelerates bone formation in both buccal side and lingual side of the scaffold.

Keywords: Osteogenesis; low-intensity collimated pulse ultrasound (LICU); low-intensity focused-pulse ultrasound (LIFU); porous SiC scaffold

Submitted Aug 14, 2019. Accepted for publication Dec 13, 2019.
doi: 10.21037/atm.2019.12.89
View this article at: http://dx.doi.org/10.21037/atm.2019.12.89

Introduction

Currently, non-invasive treatment has been a hot topic in the field of orthopedics. Low-intensity pulse ultrasound (LIPUS) is a form of mechanical energy that is transmitted through living tissues as acoustic pressure waves. The United States Food and Drug Administration has approved the use of LIPUS for the treatment of fresh fractures and fracture nonunion (1,2). As a non-invasive treatment, LIPUS has been shown to accelerate fracture healing and repair bone defects by promoting callus formation and stimulating osteogenesis, and its safety and cost-effectiveness have been confirmed (3,4).

Low-intensity collimated pulse ultrasound (LICU) and low-intensity focused-pulse ultrasound (LIFU) are

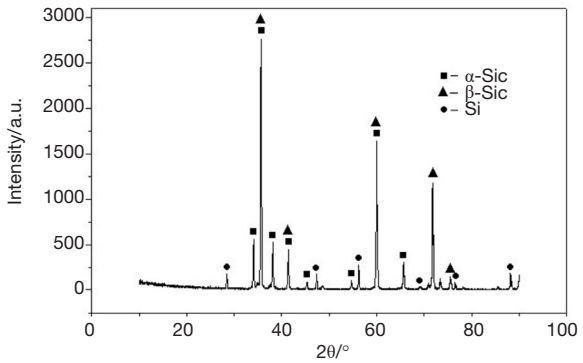

Figure 1 XRD image of the porous SiC scaffold. XRD, X-ray diffraction; SiC, silicon carbide.

two different forms of LIPUS. LICU is a collimated beam, which is emitted by a transducer into a medium for the treatment. Many studies have shown that LICU can promote the ingrowth, proliferation and early differentiation of osteoblasts in scaffold materials, improving the bone formation (5-7). LIFU is a focused acoustic beam, which has several advantages including irradiation site controllability, strong penetration and low energy attenuation. It has been reported that LIFU can significantly improve the reconstruction of bone defects through enhancing cell proliferation at the defect site (8). LIFU is also effective in the treatment of spinal cord injury (9), neuromodulation (10) and neuromuscular rehabilitation (11).

In this study, the effects of LICU and LIFU on the osteogenesis in the porous silicon carbide (SiC) scaffold implanted in the rabbit mandible were compared. First, temperature at the subcutaneous and subperiosteal tissues was measured during the LICU and LIFU, aiming to confirm the safety of above two treatments. Then, the porous SiC scaffolds were implanted into the rabbit mandible, and the bone ingrowth quantity, bone maturity and bone ingrowth depth under the LICU or LIFU were evaluated at different time points and compared.

Methods

Experimental materials

The porous SiC scaffold was prepared in the Institute of Metal Research, Chinese Academy of Sciences (Shenyang, China) according to the protocol reported previously (12). The characteristics of porous SiC scaffold are as follows: pore size, 800–1,000 μm; porosity, 70–80%; blind hole rate, <1%; compression strength, 30 MPa; elastic modulus, 20 GPa. The materials were sized 10×5×4 mm^3, ultrasonically cleaned, autoclaved (134 ℃/0.21 MPa) and prepared for use. The crystalline structure of the scaffold was evaluated by X-ray diffraction (XRD, D/max-2500PC, Rigaku) (*Figure 1*).

Experimental animals

Thirty-three adult male Japanese white rabbits (No. SYXK LIAO2008-0005) aged 6 months and weighing 2.8–3.1 kg were used in this study. The rabbits were individually housed in an unrestricted cage and fed *ad libitum*. These healthy rabbits were allowed to accommodate to the environment for 1 week before experiment. This study was approved by the Animal Ethics Committee of China Medical University.

Subcutaneous and subperiosteal temperatures during LICU and LIFU

Before surgery, six rabbits were intramuscularly anesthetized with 3% pentobarbital at 3 mL/kg (Tianwudr, Tianjin, China). A 1–2 cm incision was made parallel to the mandible, and a thermocouple probe was inserted into the subcutaneous or subperiosteal tissues for the measurement of temperature. The room temperature served as the initial temperature. Ultrasound treatment lasted for 20 min with an ultrasound therapeutic system (Chongqing Haifu Medical Technology Co. Ltd. China), and the temperature was monitored continuously. The parameters of LICU were as follows: frequency, 1.5 MHz; intensity, 30 mW/cm^2; pulse width, 200 μs; pulse repetition, 1 kHz. The parameters of LIFU were as follows: frequency, 1.5 MHz; intensity, 300 mW/cm^2; pulse width, 200 μs; pulse repetition, 1 kHz; focal spot size, 10 mm × 8 mm; focal distance, 8 mm.

Surgical implantation and LIPUS treatment

Before surgery, 27 rabbits were intramuscularly anesthetized with 3% pentobarbital at 3 mL/kg, and 2% lidocaine (Tianwudr) at 0.3 mL/kg was injected subcutaneously for local anesthesia (13). The surgical sites were parallel to the mandible and the skin, fascia and periosteum were exposed via a 3–4 cm incision using the sterile surgical technique. A rectangular defect (10×5×4 mm^3) was created by drilling into the mandibles according to a template. The implant was then gently pressed into the defect, and maintained in close and steady contact with the bone. The animals were intramuscularly injected with penicillin at 1,670 U/mg

(Tianwudr) for 3 days after implantation. These animals were randomly divided into three groups: LICU group, LIFU group and control group (sham irritation with the generator power-off). The LICU or LIFU treatment was initiated 24 h after implantation and lasted for 20 min, once daily. The parameters of LICU and LIFU were above mentioned. At each time point (3, 6 and 9 weeks after implantation), three animals were sacrificed and the implant material and approximate 1-cm surrounding bone were collected. The specimens were fixed in 4% paraformaldehyde for 1 week at 4 ℃.

Preparation of hard tissue sections

After rinsing with running water for 24 h, the specimens were dehydrated in a series of ethanol solutions (70–100%) and then embedded in methyl methacrylate and dibutyl phthalate solution. The tissue blocks were sectioned longitudinally along the long axis in a diamond-saw microtome (LeicaSP1600, Leica Microsystems, Wetzlar, Germany), and 70–80 μm sections were obtained. Each section was subsequently ground to a thickness of 30–40 μm with the sequential use of #800, #1000, #1200, and #2000 sand papers. There were 3 specimens in each group. The central three sections of each specimen were selected to ensure the comparability among specimens, and five fields were randomly selected from each section for the assessment of bone tissue morphology and quantitative analysis.

Methylene blue-acid fuchsin staining

Sections were stained with methylene blue-acid fuchsin, and the osteogenesis and bone maturity were assessed under a light microscope (OlympusBX 51+DP71, Tokyo, Japan). The bone mass was determined using the image analysis software (Image-Pro Plus 6.0, Media Cybernetics, Rockville, MD, USA). The parameters (brightness, contrast ratio, white balance, exposure time, etc.) were constant during the whole histological examination.

Micro-CT (M-CT) test

Observation of M-CT scanning: The M-CT (Y. Cheetah, Germany) images and data were evaluated using image analysis software (Mimics 16.0, Materialise, Leuven, Belgium). There were 3 specimens in each group. Scanning was performed along the long axis of the implant. A region of interest (ROI) was generated, consisting of bone with material implantation. The M-CT value was chosen to differentiate among materials, host bone and residual pores (including soft tissues) in each specimen, and then reconstruction was performed.

Quantitative analysis of M-CT

(I) Mean pore occupancy fraction (POF): POF was measured as follow: POF = Vbone/(Vbone+Vresidual pore) ×100%, where Vbone is the bone volume and Vresidual pore is the total pore volume (14).

(II) POF in different directions: data were imported to the Mimics software as shown in 2.7.1. Mimics software separated images from a continuous sectional image and generated two masks which were the "bone tissue and material" mask and "20 μm (thickness of M-CT slices) positioning" mask according to the different thresholds. The mask had been generated by 3D reconstruction from different directions (distal to mesial, top to bottom, buccal to lingual) of the material (10×5×4 mm^3). The POF of each M-CT slice was measured by Boolean operations (*Figure 2*).

Statistical analysis

Data are expressed as the mean ± standard deviation (SD), and one-way ANOVA was used to compare the quantity and structure of bone among groups, followed by Tukey-Kramer test for pairwise comparison. Statistical analysis was done with the SPSS version 21.0 (IBM SPSS Statistics for Windows, Armonk, NY, USA). A value of P less than 0.05 was considered statistically significant.

Results

Subcutaneous and subperiosteal temperatures during LICU and LIFU

For LICU, the subcutaneous and subperiosteal temperatures in all three rabbits varied within 1 ℃, and the change in the subcutaneous and subperiosteal temperature was 0.9 ℃ (*Figure 3A*) and 0.6 ℃ (*Figure 3B*), respectively. For LIFU, the subcutaneous and subperiosteal temperatures in all three rabbits also varied within 1 ℃, and the and the change in the subcutaneous and subperiosteal temperature was within 0.9 ℃ (*Figure 3C*) and 0.8 ℃ (*Figure 3D*), respectively.

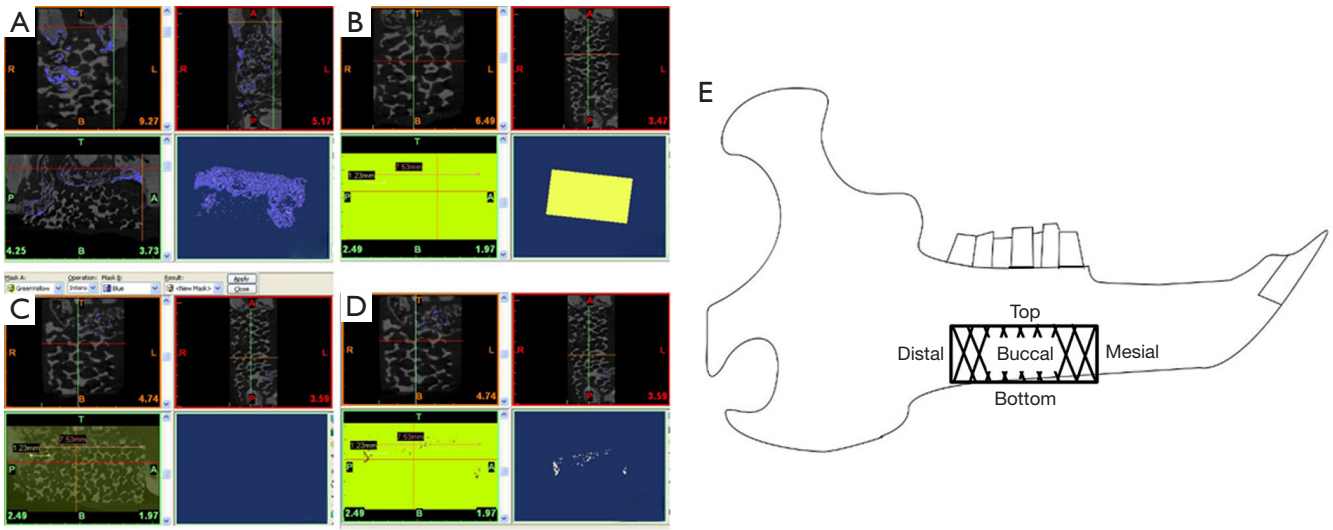

Figure 2 Schematic diagram of each bone tissue mask and different directions of material. (A) Bone tissue and material mask; (B) 20 μm (thickness of M-CT slices) positioning mask; (C) Boolean operations between two masks (intersects); (D) bone tissue mask; (E) different sections of the material.

Methylene blue–acid fuchsin staining

After methylene blue-acid fuchsin staining, the total bone mass in the LICU and LIFU groups was significantly greater than in the control group, and the mass in the LIFU group was significantly more than in the LICU group at 3, 6 and 9 weeks after implantation (P<0.05) (*Figure 4*).

M-CT

The new bone volume increased over time in the three-dimensionally (3D) reconstructed images of the mesial, distal, and upper areas of the material. The mean POF of the material also increased over time in each group. However, the mean POF in the LIPUS group was significantly greater than in the control group (P<0.05), and that in the LIFU group was markedly greater than in the LICU group at 3, 6 and 9 weeks after implantation (P<0.05) (*Figure 5*).

Distal-to-mesial

The amount of new bone increased over time in all three groups. At 3, 6 and 9 weeks after implantation, significantly more new bone was observed in both ultrasound-treated groups as compared to the control group (P<0.05); at 3 and 6 weeks after implantation there was no marked difference in the bone mass between the LIPUS groups (3 w: P=0.18; 6 w: P=0.26); at 9 weeks after implantation, significantly more new bone was noted in the LIFU group than in the LICU group (P<0.05).

At 3 weeks after implantation, there was significantly more bone in the mesial and distal areas of the implant than in the middle area in all groups (P<0.05). The curve became less steep at 6 and 9 weeks after implantation; the amount of new bone in the middle of the implant increased, but there was still more bone mass at both ends of the implants than in the middle (*Figure 6*).

Top-to-bottom

The amount of new bone increased over time in all three groups. At 3, 6 and 9 weeks after implantation, there was significantly more new bone in the ultrasound-treated groups than in the control group (P<0.05); at 3 and 6 weeks after implantation, there was no marked difference between LIPUS groups (3 w: P=0.21, 6 w: P=0.28); at 9 weeks after implantation, there was significantly more new bone in the LIFU group than in the LICU group (P<0.05).

At 3, 6 and 9 weeks after implantation, there was significantly more bone at the top than in the middle (P<0.05), with the least bone at the bottom of the implant in all groups (*Figure 7*).

Buccal-to-lingual

The amount of new bone increased over time in all three groups. At 3, 6 and 9 weeks after implantation, there was

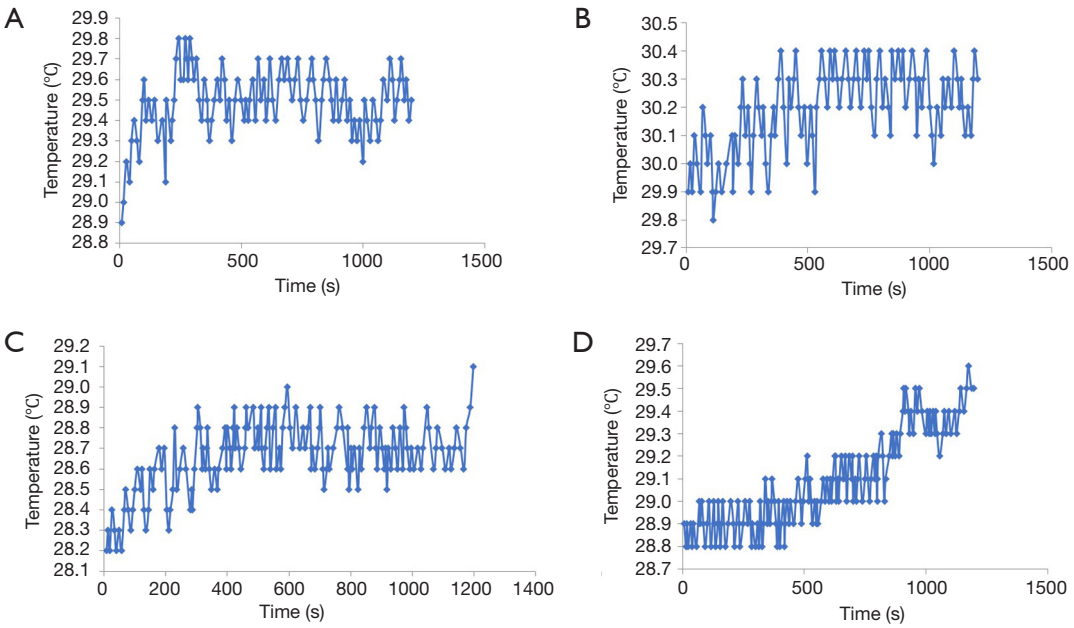

Figure 3 Temperature changes during LIPUS. (A) Subcutaneous temperature changes during LICU; (B) subperiosteal temperature changes during LICU; (C) subcutaneous temperature changes during LIFU; (D) subperiosteal temperature changes during LIFU. The temperature variations in both LICU and LIFU groups were no more 1 ℃. LIPUS, low-intensity pulse ultrasound; LICU, low-intensity collimated pulse ultrasound; LIFU, low-intensity focused-pulse ultrasound.

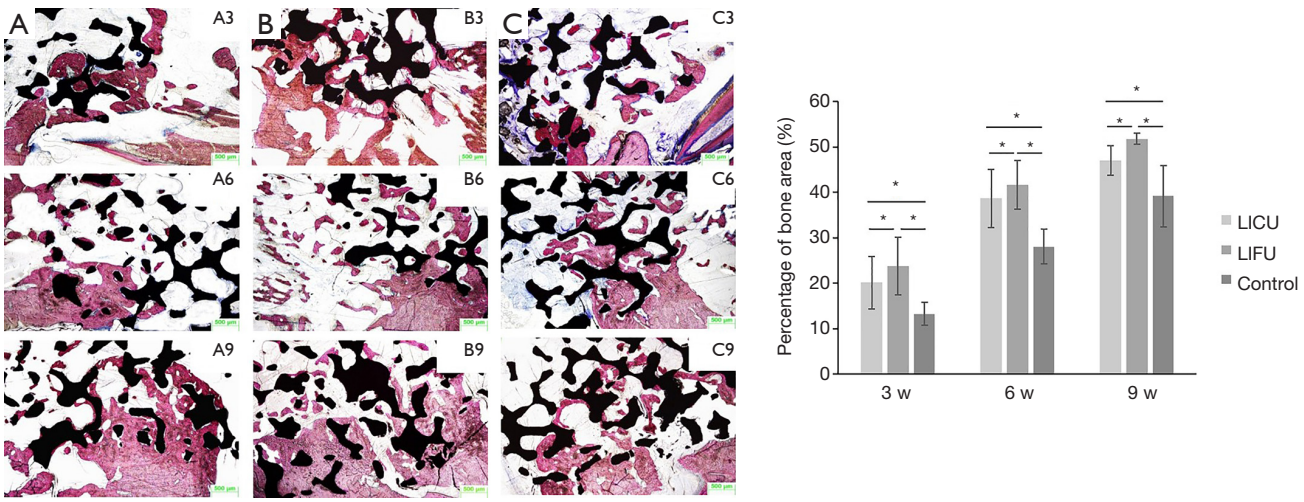

Figure 4 Photomicrograph of scaffolds (40×) and analysis of bone area after methylene blue-acid fuchsin staining. (A) LICU group; (B) LIFU group; (C) control group; 3: 3 weeks after implantation; 6: 6 weeks after implantation; 9: 9 weeks after implantation. More bone formation was observed in the LICU and LIFU groups than in the control group at the same time point; a significantly greater area of bone was noted in the LIFU group than in the LICU group. *, P<0.05. LICU, low-intensity collimated pulse ultrasound; LIFU, low-intensity focused-pulse ultrasound.

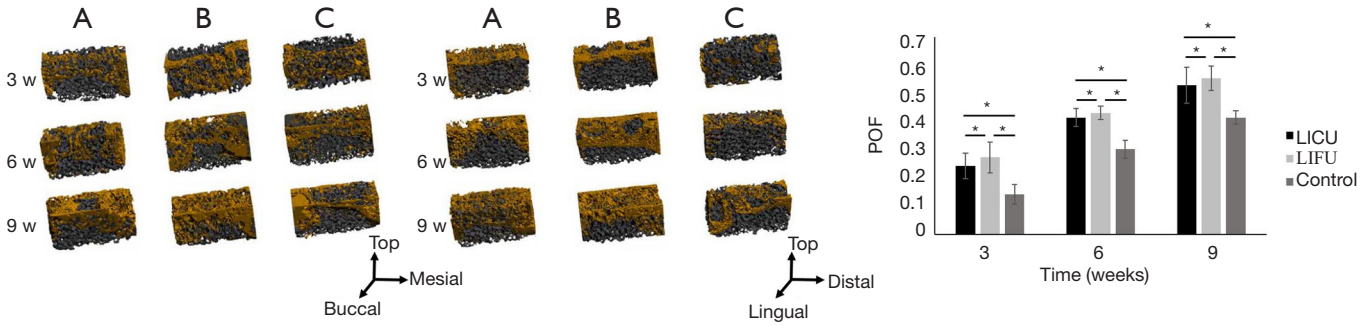

Figure 5 Three-dimensionally (3D) reconstructed images from the buccal and lingual surface and the mean POF at 3, 6, and 9 weeks after implantation. (A) LICU group; (B) LIFU group; (C) control group; black: SiC; yellow: new bone. In 3D reconstructed images, the new bone volume in the LIPUS group was greater than in the control group, and the area in the LIFU group was larger than in the LICU group. The mean POF in the LIPUS group was also significantly greater than in the control group, and the POF in the LIFU group was significantly greater than in the LICU group. *, P<0.05. POF, pore occupancy fraction; LICU, low-intensity collimated pulse ultrasound; LIFU, low-intensity focused-pulse ultrasound; SiC, silicon carbide.

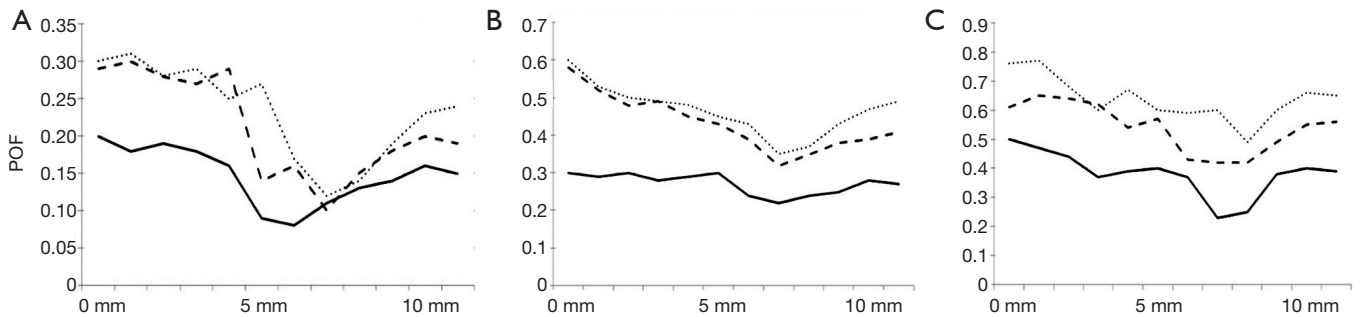

Figure 6 Cartograms of new bone from distal end to mesial end. The distal ends of the scaffolds are indicated as 0 mm, and the mesial ends are indicated as 10 mm. (A) 3 weeks after implantation; (B) 6 weeks after implantation; (C) 9 weeks after implantation; ---, LICU group; …, LIFU group; —, control group; 0 mm →10 mm: distal to mesial.

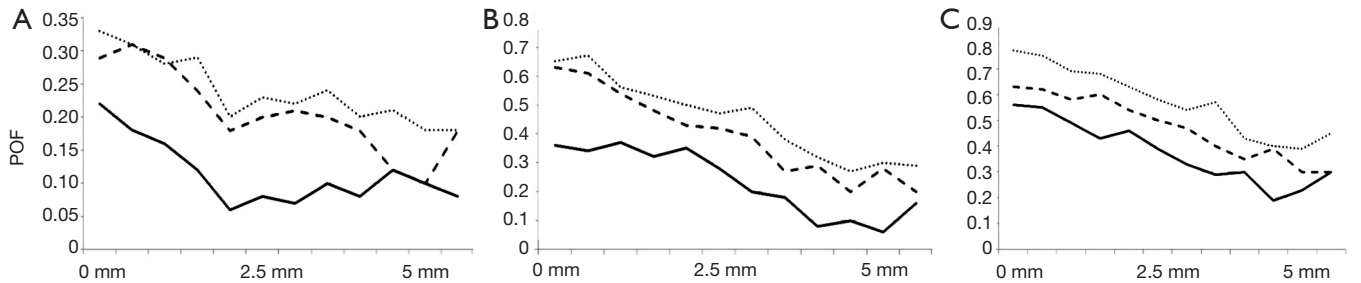

Figure 7 Cartograms of new bone from top to bottom. The top of the scaffolds is indicated as 0 mm, and the bottom is indicated as 5 mm. (A) 3 weeks after implantation; (B) 6 weeks after implantation; (C) 9 weeks after implantation; ---, LICU group; …, LIFU group; —, control group; 0 mm →5 mm: top to bottom.

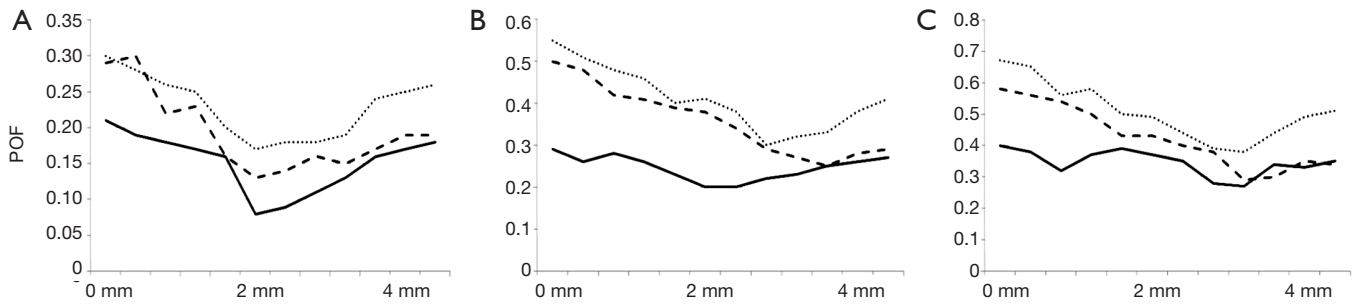

Figure 8 Cartograms of new bone formation from buccal to lingual. The buccal end of the scaffolds is indicated as 0 mm, and the lingual end is indicated as 4 mm. (A) 3 weeks after implantation; (B) 6 weeks after implantation; (C) 9 weeks after implantation; ---, LICU group; …, LIFU group; —, control group; 0 mm →4 mm: buccal to lingual.

significantly more new bone in the ultrasound-treated groups than in the control group (P<0.05), and the amount of new bone in the LIFU group was significantly more than in the LICU group (P<0.05).

In the control group, the new bone in the buccal area of the implant was almost the same to the middle and lingual areas of the implant at 3, 6 and 9 weeks after implantation. The curve was flat in the whole study period. In the buccal area, there was significantly more new bone in the LIPUS group than in the control group at the same time (P<0.05). As depth increased (to lingual), the amount of bone in the LICU group was gradually close to that in the control group, but there was significantly more new bone in the LIFU group than in the LICU group and the control group (P<0.05) (*Figure 8*).

Discussion

LIPUS treatment is an emerging physical therapy for the bone, nerve, and muscle disorders (15). Available studies have confirmed that it can suppress inflammation, promote osteogenesis and facilitate the ossification of hypertrophic chondrocytes (16,17). This study investigated and compared the effects of LICU and LIFU on the bone formation in rabbits. The intensity of LICU was 30 mW/cm^2 and the intensity of LIFU was 300 mW/cm^2, both of which are commonly used in clinical practice and studies and have been widely recognized as safe (18-20). In this study, subcutaneous and subperiosteal temperatures were measured continuously during the 20-min LICU or LIFU treatment. Our results showed the subcutaneous and subperiosteal temperatures remained relatively stable and their changes were less than 1 ℃. This suggests no damage to cells or tissues (21,22).

As shown in our study, the new bone area in the LIPUS groups was greater than in the control group (P<0.05). Although the mechanism underlying the therapeutic effects of ultrasound is still poorly understood, experiments have shown that LIPUS can promote osteoblast differentiation and bone formation. Cao *et al.* (7) have confirmed that LIPUS promotes osteoblast differentiation and enhances bone ingrowth and bone formation in porous Ti6Al4V scaffolds. Feng *et al.* (5) found that both 1 and 3.2 MHz LIPUS promoted the osteoblast differentiation *in vitro* and enhanced bone maturity in the porous Ti64 scaffolds implanted into rabbit mandibular defects. Our results also confirmed that LIPUS enhances bone formation in the porous SiC scaffolds.

Studies have shown both LICU and LIFU (two different forms of LIPUS) are able to promote osteogenesis. Wu *et al.* (6) found that LICU facilitated the cellular ingrowth and enhanced the proliferation and early differentiation of osteoblasts in the porous SiC scaffolds. Short-term (2-wk) LICU therapy initiated trabecular bone repair and regeneration in the large trabecular bone defects, whereas cortical bone remained in the initial non-mineralization stage (23). LIFU can also improve the re-ossification through enhancing cell proliferation in the calvarial defect sites (8). However, little is known about the therapeutic effects of LICU and LIFU on the large bone defects. In the present study, results showed the area of bone formation in the LIFU group was greater than in the LICU group, especially in the lingual area of the scaffold (P<0.05). The penetration depth of LIPUS is very important for therapeutic efficacy. The energy of LICU undergoes attenuation to a certain extent as it passes through the skin, subcutaneous tissues, fascia and muscle, and thus whether the ultrasound with required energy can

reach the target site is unclear. LIFU has low energy and pulse as in LICU, but has better penetration capability. The intensity of LIFU becomes stronger when it is close to the focal spot, which is sized 10 mm × 8 mm, and thus LIFU is able to encompass the whole scaffold (10×5×4 mm^3). The focal distance of LIFU is 8 mm, almost the same as the sum of the depths of the skin (1 mm), subcutaneous tissue (1 mm), muscle (1–2 mm) and scaffold (5 mm). Hence, the energy of LIFU reaching the lingual side of the material is sufficient for the treatment, and more bone formation was observed at lingual side in the LIFU group than in the LICU group. These findings indicate that LIFU accelerates bone formation not only in the buccal area but also in the lingual area of the implant.

Our study indicates ultrasound treatment after implantation of scaffolds is more effective for the large bone defects and provides experimental evidence on the clinical treatment of large bone defects. There were still limitations in this study. Only short-term effectiveness was evaluated, and the optimal parameters of ultrasound and the scaffold should be determined before the clinical application.

Conclusions

Both LIFU and LICU effectively promote bone formation. However new bone formation in the mesial, distal, top, and lingual areas of the implants in the LIFU group are greater than in the LICU group and the control group, especially in the lingual area of the scaffold.

Acknowledgments

We thank Professor Zhang Jingsong at the Institute of Metal Research, Chinese Academy of Sciences for his support with the materials.
Funding: This study was supported by the National Natural Science Foundation of China (NSFC) (No. 81870811) and Natural Science Foundation of the Higher Education Institutions of Liaoning Province (No. LQNK201722).

Footnote

Conflicts of Interest: *The authors have no conflicts of interest to declare*.

Ethical Statement: The authors are accountable for all aspects of the work in ensuring that questions related to the accuracy or integrity of any part of the work are appropriately investigated and resolved. The experiments were approved by the Animal Ethics Committee of China Medical University (No. 2018007).

References

1. Rockville MD. US Food and Drug Administration (FDA): Sonic Accelerated Fracture Healing System (SAFHS), Model 2A: Summary of Safety and Effectiveness. Premark et Approval P900009, Exogen, Inc. US Food and Drug Administration October 5.1994.
2. Rockville MD. US Food and Drug Administration (FDA): Exogen 2000, 3000, or Sonic Accelerated Fracture Healing System (SAFHS): Summary of Safety and Effectiveness. Premarket Approval P900009/Supplement 6. Exogen, Inc. US Food and Drug Administration February 22, 2000.
3. Duarte LR. The stimulation of bone growth by ultrasound. Arch Orthop Trauma Surg 1983;101:153-9.
4. Ikai H, Tamura T, Watanabe T, et al. Low-intensity pulsed ultrasound accelerates periodontal wound healing after flap surgery. J Periodontal Res 2008;43:212-6.
5. Feng L, Liu X, Cao H, et al. A Comparison of 1- and 3.2-MHz Low-Intensity Pulsed Ultrasound on Osteogenesis on Porous Titanium Alloy Scaffolds: An In Vitro and In Vivo Study. J Ultrasound Med 2019;38:191-202.
6. Wu L, Lin L, Qin YX. Enhancement of cell ingrowth, proliferation, and early differentiation in a three-dimensional silicon carbide scaffold using low-intensity pulsed ultrasound. Tissue Eng Part A 2015;21:53-61.
7. Cao H, Feng L, Wu Z, et al. Effect of low-intensity pulsed ultrasound on the biological behavior of osteoblasts on porous titanium alloy scaffolds: An in vitro and in vivo study. Mater Sci Eng C Mater Biol Appl 2017;80:7-17.
8. Jung YJ, Kim R, Ham HJ, et al. Focused low-intensity pulsed ultrasound enhances bone regeneration in rat calvarial bone defect through enhancement of cell proliferation. Ultrasound Med Biol 2015;41:999-1007.
9. Song Z, Ye Y, Zhang Z, et al. Noninvasive, targeted gene therapy for acute spinal cord injury using LIFU-mediated BDNF-loaded cationic nanobubble destruction. Biochem Biophys Res Commun 2018;496:911-20.
10. Bowary P, Greenberg BD. Noninvasive Focused Ultrasound for Neuromodulation: A Review. Psychiatr Clin North Am 2018;41:505-14.
11. Sungjin O, Dong Hwee K, Inchan Y. Low-intensity focused ultrasound stimulator using focal depth controller for improved targeting in neuromuscular rehabilitation. Conf Proc IEEE Eng Med Biol Soc 2017;2017:209-12.

12. Wu L, Yuan Y, Hao FY, et al. The effects of SiC foams on cell proliferation and differentiation in primary osteoblasts. J Hard Tissue Biol 2015;24:37.
13. Liu XH, Wu L, Ai HJ, et al. Cytocompatibility and early osseointegration of nanoTiO2-modified Ti-24 Nb-4 Zr-7.9 Sn surfaces. Mater Sci Eng C Mater Biol Appl 2015;48:256-62.
14. Jingyu W, Lin W, Yong G, et al. Experimental study on the osseointegration of foam TiC/Ti composites. Biomed Mater 2013;8:045001.
15. Liang C, Yang T, Wu G, et al. Therapeutic effect of low-intensity pulsed ultrasound on temporomandibular joint injury induced by chronic sleep deprivation in rats. Am J Transl Res 2019;11:3328-40.
16. Kusuyama J, Nakamura T, Ohnishi T, et al. Low-intensity pulsed ultrasound promotes bone morphogenic protein 9-induced osteogenesis and suppresses inhibitory effects of inflammatory cytokines on cellular responses via Rho-associated kinase 1 in human periodontal ligament fibroblasts. J Cell Biochem 2019;120:14657-69.
17. Sekino J, Nagao M, Kato S, et al. Low-intensity pulsed ultrasound induces cartilage matrix synthesis and reduced MMP13 expression in chondrocytes. Biochem Biophys Res Commun 2018;506:290-7.
18. Fung CH, Cheung WH, Pounder NM, et al. Effects of different therapeutic ultrasound intensities on fracture healing in rats. Ultrasound Med Biol 2012;38:745-52.
19. Kristiansen TK, Ryaby JP, McCabe J, et al. Accelerated healing of distal radial fractures with the use of specific, low-intensity ultrasound. A multicenter, prospective, randomized, double-blind, placebo-controlled study. J Bone Joint Surg Am 1997;79:961-73.
20. Wu J, Chen D, Langevin HM, et al. Interaction between parallel polymer fibers insoni ficated by ultrasound of low/mild intensity: an analytical theory and experiments. Ultrasonics 2012;52:417-21.
21. Nema N. Acoustic output measurement standard for diagnostic ultrasound equipment. Revision 3 NEMA UD 2, 2004.
22. Chang WH, Sun JS, Chang SP, et al. Study of thermal effects of ultrasound stimulation on fracture healing. Bioelectromagnetics 2002;23:256-63.
23. Liu J, Li X, Zhang D, et al. Acceleration of Bone Defect Healing and Regeneration by Low-Intensity Ultrasound Radiation Force in a Rat Tibial Model. Ultrasound Med Biol 2018;44:2646-54.

Cite this article as: Liu X, Hu Y, Wu L, Li S. Effects of collimated and focused low-intensity pulsed ultrasound stimulation on the mandible repair in rabbits. Ann Transl Med 2020;8(4):98. doi: 10.21037/atm.2019.12.89

